Title
EXPERIMENTS AT HIGH VOLTAGE ELECTRON MICROSCOPY

Author
Thomas, Gareth

Publication Date
1967-09-01

University of California

Ernest O. Lawrence Radiation Laboratory

EXPERIMENTS AT HIGH VOLTAGE ELECTRON MICROSCOPY

Gareth Thomas

September 1967

Berkeley, California

Submitted to Phil. Mag.

UCRL-17842
Preprint

UNIVERSITY OF CALIFORNIA

Lawrence Radiation Laboratory
Berkeley, California

AEC Contract No. W-7405-eng-48

EXPERIMENTS AT HIGH VOLTAGE ELECTRON MICROSCOPY

Gareth Thomas

September 1967

EXPERIMENTS AT HIGH VOLTAGE ELECTRON MICROSCOPY

Gareth Thomas

Inorganic Materials Research Division, Lawrence Radiation Laboratory, and Department of Mineral Technology, College of Engineering, University of California, Berkeley, California

September 1967

ABSTRACT

Experiments have been performed to investigate the useful thickness limits for electron transmission under routine operating conditions for silicon and stainless steel. The criterion adopted for this limit was that thickness at which fringe contrast at faults was destroyed by absorption. The results indicate a roughly linear behavior of this limit at intermediate voltages, then falling off, but less rapidly than a $(v/c)^2$ law. At 1 meV foils of silicon $\sim 9\mu$ and stainless steel $\sim 2\mu$ thick are adequately transparent for observing defects. The ultimate thickness limit is determined by contrast and chromatic aberration.

Measurements of the mean absorption parameter vs voltage in silicon showed a non-linear behavior above about 100 kV. This result is attributed to the effect of many beams which cannot be avoided when using the wedge fringe method at high energies.

It has been found that simultaneous reflections can lower the useful thickness limit by as much as 25% due to an increase in apparent absorption.

An application of UHV microscopy to the study of interfaces between epitaxial silicon and its substrate is described.

§ 1. INTRODUCTION

It is well recognized that the main advantage of high voltage electron microscopy is the ability to observe thick materials (Dupouy and Perrier 1962-1964, Cosslett 1962, Fujita et al. 1967, Uyeda and Nonoyama 1967). Consequently, it becomes possible to examine materials not easily observed in conventional 100 kV instruments (e.g. the heavy elements such as W, U) and to be more certain that substructural features in foils are representative of those in bulk material.

Very little information is available on the transparency limits of crystals. Uyeda and Nonoyama (1967) investigated molybdenite films and utilized the criterion that the useful thickness limit corresponds to diffraction patterns which contain only Kikuchi bands. Their results did not enable any conclusions to be drawn regarding the voltage dependence of the maximum transparancy thickness, but dislocations could be observed in foils 3μ thick at 500 kV.

Fujita et al. (1967) carried out metallurgical investigations including a determination of the transmissive power for aluminum and stainless steel based on measurements of the mean absorption coefficient from wedge fringe profiles. They found that aluminum is about 2.3 times more transmissive than iron and showed that static images of dislocations could be obtained from foils of about 8μ (Al) and 2μ (Fe) thick at 500 kV. Hashimoto (1964) measured the energy dependence of absorption in aluminum and Dupouy et al. (1965) measured the transmissive power of MgO and found deviations from the predicted dependence on electron velocity (Fujiwara 1962, Howie 1962) which were later explained in terms of multiple diffraction (Goringe et al.

1966, Metherell and Whelan 1967). These preliminary results indicate that the transparency of crystals is determined by the absorption coefficients, in general agreement with theory (Hirsch 1962, Hashimoto et al. 1962), and that the limiting factor in terms of image quality is the contrast and chromatic aberration resulting from inelastic scattering processes leading to energy losses which occur as the beam penetrates the foil.

The present investigation was initiated to obtain data on the useful thickness limits for materials of differing absorbing power, viz., silicon and stainless steel, under constant known diffracting conditions and routine microscope operations.

§ 2. EXPERIMENTAL

Foils of single crystal silicon and polycrystalline austenitic stainless steel were prepared in the usual way. Areas of foils were chosen in which stacking faults or twins were present so that the true foil thickness could be obtained from the projected widths of the fault traces. The particular (111) variant of the fault plane was uniquely known from the precise orientation of the foil given by the Kikuchi pattern (Levine et al. 1966) and was checked in some cases by dark field experiments at $s \neq 0$ (Bell and Thomas 1965).

The criterion adopted for the thickness limit in these experiments was that thickness at which fringe contrast was destroyed because of absorption (absorption thickness limit, ATL). This method gives a visibility criterion which is determined chiefly by the mean absorption coefficient for given contrast (diffraction) conditions. In each case a systematic

<111> reflection was chosen with the foil oriented between [110] and [123] to avoid exciting simultaneous reflections as far as possible, since it has been found that simultaneous reflections produce an apparent increase in absorption of order 25% (Ayroles and Mazel 1967). The experiments were conducted in the following way. An area was selected at high voltage where fringe contrast was resolved. The voltage was then reduced until fringes could no longer be resolved. Care was taken to readjust the tilt of the foil to maintain s = 0 conditions as closely as possible. Adjustments are necessary due to the increase in Bragg angle as the voltage is lowered. A 30μ objective aperture was used in each case and a maximum beam current of 5μA was employed. Photographs were taken under normal exposure conditions with defocussed second condenser. Bright field and dark field images and selected area diffraction patterns were recorded in each case and near the limit of fringe resolution several photographs were obtained at different objective focussing and tilt adjustments; the best examples were used for measurements.

The experiments at 100 kV were done on a Siemens microscope and the majority of the high voltage experiments were done using the Cambridge 750 kV microscope and the Toulouse 1.2 meV microscope. Some preliminary experiments on wedge fringes were carried out using the Hitachi 500 kV microscope.

§ 3. RESULTS AND DISCUSSION

3.1. Thickness Limits

Figure 1 shows a series of experiments done on silicon which illustrates the method employed. This case is for a foil ∿ 3μ thick and it can be seen that at 300 kV very few fringes are resolved. Figure 2 shows densitometer traces of the fringe profiles and this illustrates the increase in absorption (decrease in width of the dynamical envelope) with decreasing voltage. Similar results apply to increasing the thickness at any given voltage.

Figure 3 shows a similar series of experiments done on stainless steel. The fringes are visible only under conditions of anomalous transmission as can be seen from the diffraction patterns of Figs. 1 and 3.

The results of these experiments are plotted in Figure 4. The values given are for images where a maximum of three outer fringes are resolvable. It can be seen that silicon is considerably more transparent than stainless steel and extrapolation to 1 meV indicates that the ATL's are of the order of 9μ for Si and 2μ for stainless steel. At the lower voltage ranges the ATL is roughly linear with voltage and then appears to fall off slightly above 500 kV, but not as rapidly as predicted by a (v/c) or a $(v/c)^2$ law. This result indicates that the visibility of the fringes is not simply dependent on the mean absorption parameter. No evidence for enhanced transmission due to the channeling phenomena discussed by Howie (1966) was detected.

3.2. Transmissive Power

Transmissive power is usually defined as the reciprocal of the mean absorption coefficient. The latter can be estimated by taking photographs of thickness extinction contours at wedge shaped crystals as described by Hashimoto et al. (1962). The values of the mean absorption distance are not affected by the size of the objective aperture (Metherell and Whelan

1967), but difficulties are encountered at high voltages due to the unavoidability of exciting many reflections.

According to the two beam dynamical theory (see e.g. Hirsch et al. 1965), the mean absorption distance ξ_o' should be proportional to the square of the electron velocity. It has been proposed that deviations from this law (observed by Dupouy et al. (1965) in MgO) are due to many-beam effects (Goringe et al. 1966). Recently Metherell and Whelan (1967) showed theoretically that when many-beam effects are considered the linear dependence of ξ_o' with v^2 for aluminum breaks down above $\sim$ 200 kV.

Figures 5a, b show bright and dark field images of wedge fringes in silicon at 1.2 meV and Fig. 5c shows the diffraction pattern. At least 120 reflections are excited to some extent. The probability of exciting many reflections increases with increasing voltage because of the decrease in Bragg angle and increase in radius of the reflecting sphere. These factors coupled with the effect of the form factor giving rise to relrods in patterns from the edges of the foil make it very difficult to avoid exciting many reflections. Because of these factors it is difficult to obtain meaningful data on absorption constants and extinction distances from wedge fringes at high voltage.

Figure 6 is a plot of the reciprocal of the mean absorption parameter $(\xi_o'/2\pi\ \xi_g)$ vs (v/c) for silicon obtained by the wedge fringe method. The value at 100 kV was obtained under good two beam [111] conditions and at higher voltages for principally systematic <111> diffraction. However, above about 300 kV it was difficult to avoid simultaneous reflections (e.g. Figure 5) and this probably accounts for the non-linear behavior of the transmissive power with v^2 in agreement with the proposals of Goringe et al. (1966) and Metherell and Whelan (1967).

3.3. Diffracting Conditions

Another effect which has been observed is that under simultaneous diffraction conditions there is a decrease in observability of fringes, i.e. an apparent increase in absorption. This effect can be seen by comparing Figs. 7a and 7b and their diffraction patterns. In Fig. 7a the orientation is such that principally systematic <111> reflections operate. After tilt-rotation towards the [110] pole simultaneous reflections have been excited and it can be seen that the intensity of the fringe contrast is lowered and that the number of visible fringes has been reduced by about 25%. These results indicate that in order to optimise visibility and transmission, it is essential to avoid exciting simultaneous reflections. In order to achieve this it is necessary to orient the foil away from poles of high symmetry and reference to the appropriate Kikuchi map facilitates these required operations. Furthermore, it is also important to use the lowest order reflections in order to maximise contrast.

3.4. Contrast and Visibility

Whilst the experiments described above enable a comparison to be made of the transmission under identical conditions, the limits shown in Figure 4 are by no means absolute thickness limits. For example, different values of ATL can be obtained by changing the diffraction conditions, since this will change the contrast at defects and will affect their visibility. The results were obtained essentially at $s = 0$ conditions, yet simple theory predicts that in bright field maximum intensity occurs at s > 0 if one utilizes anomalous absorption, but the condition s = 0 should still be maintained for maximum dark field intensity. However, these rules must break down under the conditions where anomalous absorption is no longer useful. Under these situations the useful image information will be limited by chromatic aberration due to the energy spread resulting from inelastic scattering within the specimen. For a given thickness the aperture dark field image shows better resolution with increasing kV due to the decrease in chromatic aberration as, e.g., Fig. 8 shows.

It has been found that dislocation images are observable even though fringe contrast has been destroyed, for example, dislocations can be adequately resolved in stainless steel 2μ thick at 1 meV. This is due to the fact that the contrast conditions for observing fault fringes and dislocation images are not the same. Figures 3 and 9 show examples of dislocation images visible when no twin boundary fringes are resolved. As expected, the dislocation images have lost their oscillatory characteristics (compare to Fig. 8), but still have adequate contrast over background to be observed. In Figure 9b the photograph was taken under extremely difficult operating conditions, viz. the contrast on the screen was very poor at a beam current of 3μA, making focusing and adjustment of optimum diffracting conditions extremely difficult. Under these conditions, which approach the maximum useful operating limit, increasing the beam current can increase brightness but not contrast, but also leads to the problem of exciting x-rays to a dangerous level. This may necessitate remote control of the experiment, which is not very convenient. Thus for routine electron microscopy, the limits given in Figure 4 can be regarded as the optimum practical operating voltages at beam currents under 5μA. The ultimate thickness is still restricted by image contrast rather than by image brightness. This is to be expected, since the effects of inelastic and incoherent scattering increase the background level to such a limit that contrast (intensity above or below background) is completely lost.

3.5. Ancillary Observations

In general, provided systematic orientations are observed, the general predictions of the simple dynamical theory of contrast are maintained at high voltage (see e.g. Hirsch et al. 1965). It has been found, for example, that the symmetry properties of fringe patterns are not changed, even if simultaneous conditions are encountered. In the latter case, complications in the detail of the image may arise, e.g. fringe doublets or triplets (see e.g. the faults in Fig. 5), and the general contrast is lowered. In any case, it is fairly easy to choose the thickness and orientation at any voltage such that essentially two beam conditions are achieved (e.g. Fig. 3c) and thereby facilitate operating at high voltage under routine conditions typical of conventional 100 kV microscopy, so that existing theory can be applied for analysis.

Hashimoto (1964, 1967) has shown that in thicker crystals the images near the top surface may be more diffuse than those of the bottom surface, particularly in dark field due to the increased chromatic aberration. This effect was explained as being due to the increased divergence of the beam in thick specimens because of inelastic scattering. In the present work no noticeable effect due to this phenomenon was observed even near the ultimate useful thickness limits (e.g. Fig. 9).

In thick specimens difficulties arise due to radiation damage, e.g.

a copper atom is displaced by electrons of $\sim$ 500 keV. Small defect clusters can be observed in thick foils after several minutes exposure to a high energy beam, particularly if the beam current exceeds $\sim$ 10μA (depending on thickness and material). Figure 10 shows examples of the typical black/white strain contrast images due to vacancy or interstitial clusters (see e.g. Harwell Conf. 1966). In Fig. 10 the defects appear to be all at the same level, since all the images have their black and white portions to the same direction. It is not known whether these defects are due to electron irradiation or to ion damage.

The useful information from the image is also limited by incoherent scattering, e.g. when the defect density is high there is considerable overlap of structure. High voltage microscopy will not therefore be useful for observing very thick foils of high dislocation density, except to indicate, as Fujita et al. (1967) have done, the thickness limit above which meaningful values of e.g. dislocation density can be measured. What high voltage microscopy can do is to facilitate observing crystals of low defect density and can bridge the gap between x-ray topography and electron microscopy.

One specific application of high voltage microscopy was undertaken viz. the study of the interface between an epitaxial layer and its substrate. Typically transistor devices of silicon are made this way and imperfections have been observed in the epitaxial layer by many workers, e.g. Booker and Unvala (1965), Finch et al. (1963). At high voltage, due to the ability to penetrate thick specimens, it is possible to prepare specimens easily so that the interface is preserved in the foil. Fig. 11

shows an example where stacking faults can be seen to originate from inclusions (not identifiable) at the interface. This result indicates the importance of impurities at the substrate surface on the structure of the deposited layer.

§ 4. CONCLUSIONS

1. The transparency thickness of crystals increases with voltage, but no conclusions could be drawn regarding the voltage dependence except that the transmissive power varies roughly as $(v/c)^2$ depending on the diffracting conditions.

2. The value of the thickness limit decreases with atomic number (and/or density) of the specimen, i.e. the more strongly absorbing the materials the lower is the useful thickness limit. Silicon, like aluminum, is highly transparent, being about a factor of four times as transparent as stainless steel. The useful thickness limits at 1 meV are approximately 9μ (Si) and 2μ (stainless steel) for the operating criterion adopted here. For stainless steel there does not appear to be a great gain in transmission above about 500 kV and more experiments are needed on heavier metals, such as tungsten and uranium, and at 1 meV and above.

3. For practical applications UHV microscopy in thick foils can be carried out most conveniently if systematic diffraction conditions are employed. Simultaneous reflections should be avoided because they cause complications in the image and increase the apparent absorption. Two beam orientations can easily be achieved by control of thickness and orientation.

4. The useful thickness limit is determined by contrast rather than brightness and the information in the image is ultimately limited by chromatic aberration due to inelastic scattering of the electrons by the specimen.

ACKNOWLEDGMENTS

This research was made possible through the kind cooperation of Professor G. Dupuoy and the staff of the Electron Optical Laboratory, Toulouse, France, and Dr. V. E. Cosslett and the electron microscopy group at the Cavendish Laboratory, Cambridge, England, who made their facilities available and to whom the author is deeply grateful. Preliminary experiments up to 500 kV were done using the Hitachi 500 kV microscope at Tokyo and Nagoya Universities, Japan, which were made possible through the assistance of Professors T. Imura and R. Uyeda. I wish to thank the United States Atomic Energy Commission for partly financing my visit to Cambridge and Toulouse and for continued financial support of our research.

REFERENCES

AYROLES, R., and MAZEL, A., 1967, J. de Microscopie, 6, 135.

BELL, W. L., and THOMAS, G., 1965, Phys. Stat. Sol., 12, 843.

BOOKER, G. R. and UNVALA, B. A., 1965, Phil. Mag., 11, 11.

COSSLETT, V. E., 1962, J. Royal Mic. Soc., 81, 1.

DUPOUY, G., and PERRIER, F., 1962, J. de Microscopie, 1, 167; 1963, Ann. Phys., 8, 251; 1964, J. de Microscopie, 3, 233; 1964, Compt. Rend., 258, 1.

DUPOUY, G., PERRIER, F., UYEDA, R., AYROLES, R., and MAZEL, A., 1965, J. de Microscopie, 4, 429.

FINCH, R. H., QUEISSER, H. J., WASHBURN, J., and THOMAS, G., 1963, J. Appl. Phys., 34, 406.

FUJITA, H., KAWASAKI, Y., FURUBAYASHI, E., KAJIWARA, S., and TAOKA, T., 1967, Jap. J. Applied Phys., 6, 214.

FUJIWARA, K., 1962, J. Phys. Soc. Japan, Suppl. B-II, 17, 118.

GORINGE, M. J., HOWIE, A., and WHELAN, M. J., 1966, Phil. Mag., 14, 217.

HARWELL CONFERENCE, Proceedings, 1966, Symposium on Nature of Small Defect Clusters (Her Majesty's Stationery Office, London).

HASHIMOTO, H., TANAKA, T., KOBAYASHI, K., SUITO, E., and IWANAGA, M., 1962, J. Phys. Soc. Japan, Suppl. B-II, 17, 170.

HIRSCH, P. B., 1962, J. Phys. Soc. Japan, Suppl. B-II, 17, 143.

HIRSCH, P. B., HOWIE, A., NICHOLSON, R. B., PASHLEY, D. W., and WHELAN, M. J., 1965, Electron Microscopy of Thin Crystals (Butterworth and Co., London).

HOWIE, A., 1962, J. Phys. Soc. Japan, Suppl. B-II, 17, 122.

HOWIE, A., 1966, Phil. Mag., 14, 223.

LEVINE, E., BELL, W. L., and THOMAS, G., 1966, J. Appl. Phys., 37, 2141.

METHERELL, A. J. F., and WHELAN, M. J., 1967, Phil. Mag., 15, 755.

UYEDA, R. and NONOYAMA, M., 1967, Jap. J. Applied Phys., 6, 557.

FIGURE CAPTIONS

Fig. 1 The same area of a silicon foil after reducing the voltage from 1200 kV to 300 kV showing the loss of fringe contrast due to absorption. a) 1200 kV; b) 1000 kV; c) 750 kV; d) 500 kV; e) 300 kV. The corresponding diffraction patterns show that the orientation remains constant with systematic [111] reflections operating. Thickness $\sim 3\mu$.

Fig. 2 Densitometric traces across the fault shown in Fig. 1.

Fig. 3 Similar to Fig. 1 for austenitic stainless steel showing bright and dark field (aperture) images; systematic <111> reflections. a) 1200 kV; b) 500 kV; c) 300 kV. Thickness $\sim 1.4\mu$. Notice that although fringe contrast is lost in c), the dislocation contrast is still good in bright field, but the quality of the dark field (aperture) image is fair due to chromatic aberration.

Fig. 4 A plot of the thickness limit for silicon and stainless steel determined from experiments such as shown in Figs. 1, 3 (systematic <111> reflections). It can be seen that the limits are not proportional to $(v/c)^2$.

Fig. 5 a) Bright field; b) aperture dark field; and c) selected area diffraction pattern of thickness extinction fringes at the edge of a silicon foil at 1.2 meV. Notice the very large number of reflections operating in addition to the principal <111> systematic. The doubling of the fault fringes is a result of simultaneous reflections.

Fig. 6 A plot of the dimensionless factor $\left[\xi_o'/2\pi\xi_g\right]$ against (v/c) for silicon; mainly systematic <111> conditions except at higher voltages (see Fig. 5).

Fig. 7 Showing a comparison of the images of stacking faults in silicon under a) principally systematic <111> conditions and b) simultaneous conditions at 1.2 meV. The sign of $\vec{g}$ has been reversed from a) to b).

Fig. 8 Comparison of a) bright field and b) dark field (aperture) g = [200], images of twin fringes and dislocations in stainless steel. Thickness ∿ 0.6μ at 1.2 meV.

Fig. 9 Bright field images of twin boundaries and dislocations in stainless steel a) 750 kV; b) 500 kV. Thickness ∿ 1.4μ. Fringes are not observable in a) but the dislocations are in good contrast. The ultimate useful thickness limit in b) is indicated by the poor contrast and resolution of the dislocations due to chromatic aberration.

Fig. 10 Showing small defect clusters in silicon after 20 minutes exposure at 700 kV; beam current ∿ 3μA.

Fig. 11 Showing the origin of stacking faults from inclusions at the substrate-epitaxial layer interface in silicon. Thickness of the layer ∿ 6-1/4μ; photographed at 1 meV.

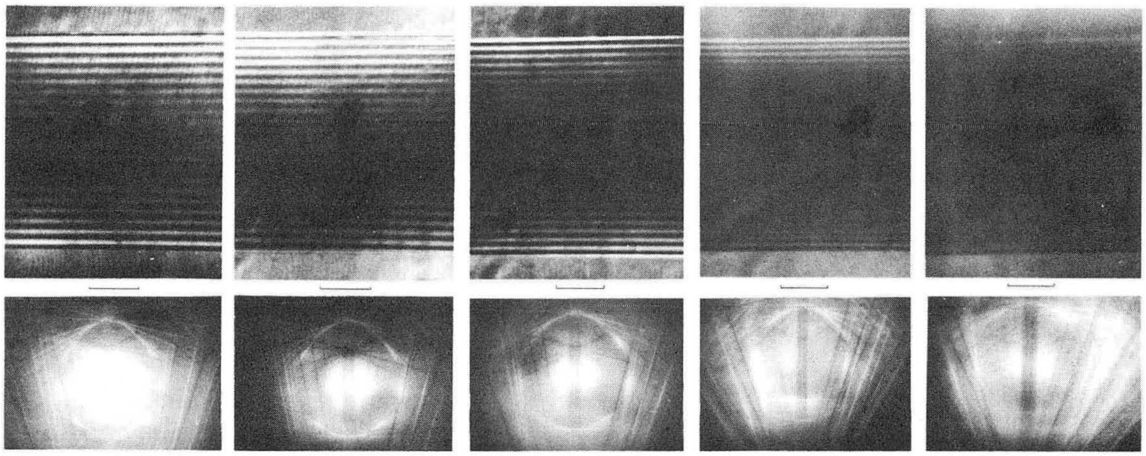

a b c d e

XBB 679-5634

Fig. 1

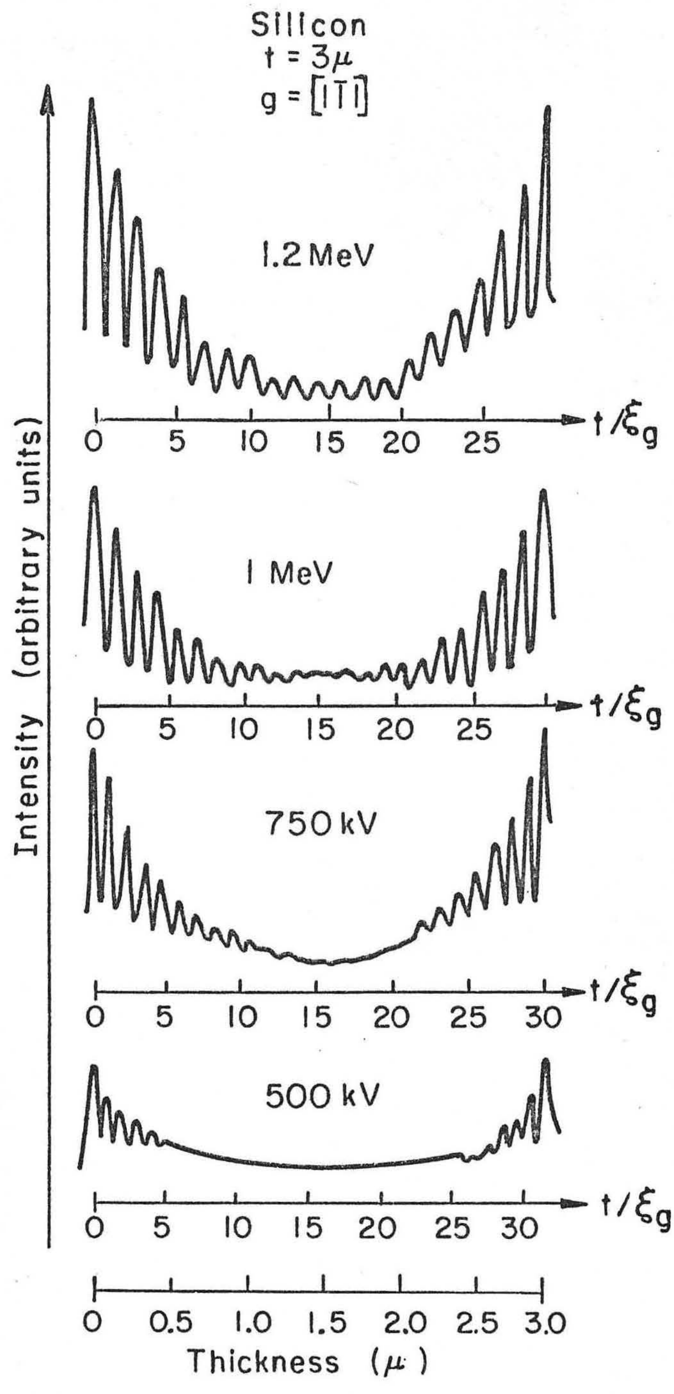

XBL678-3732

Fig. 2

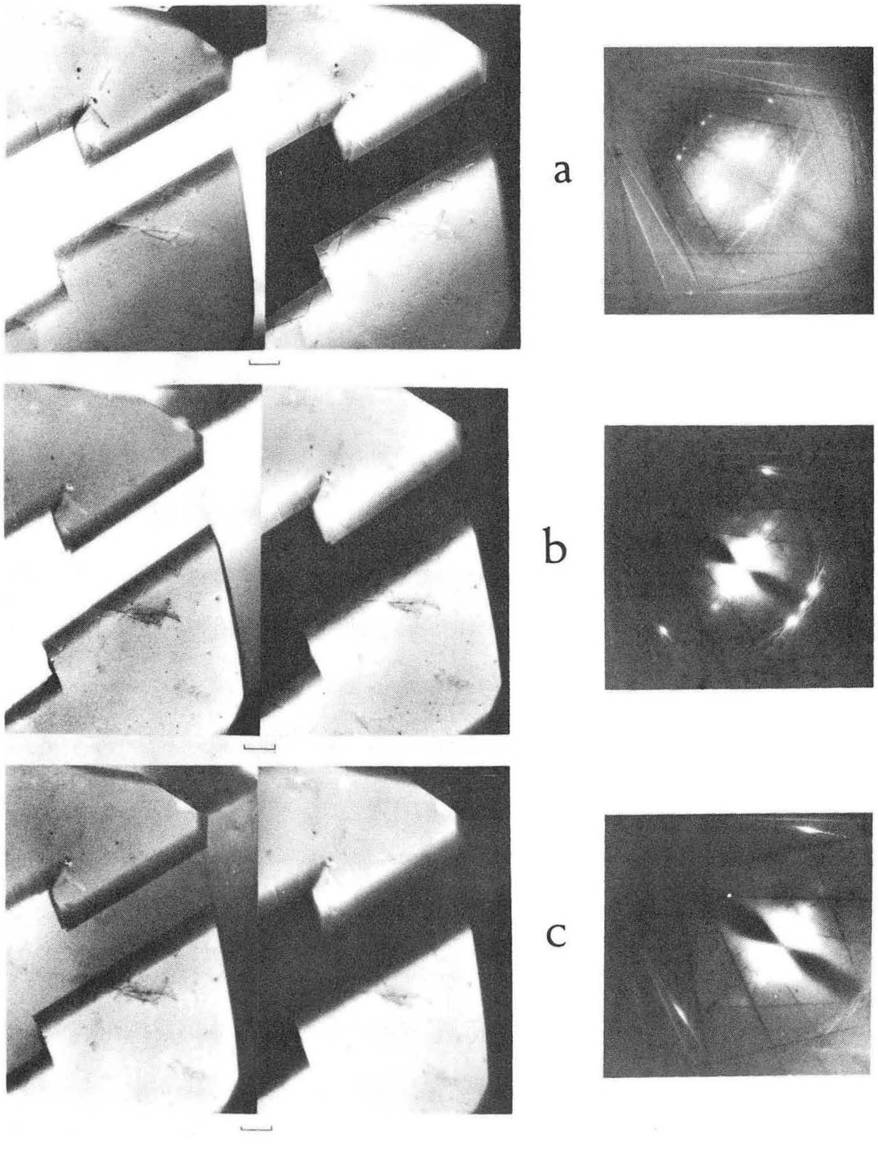

XBB 679-5632

Fig. 3

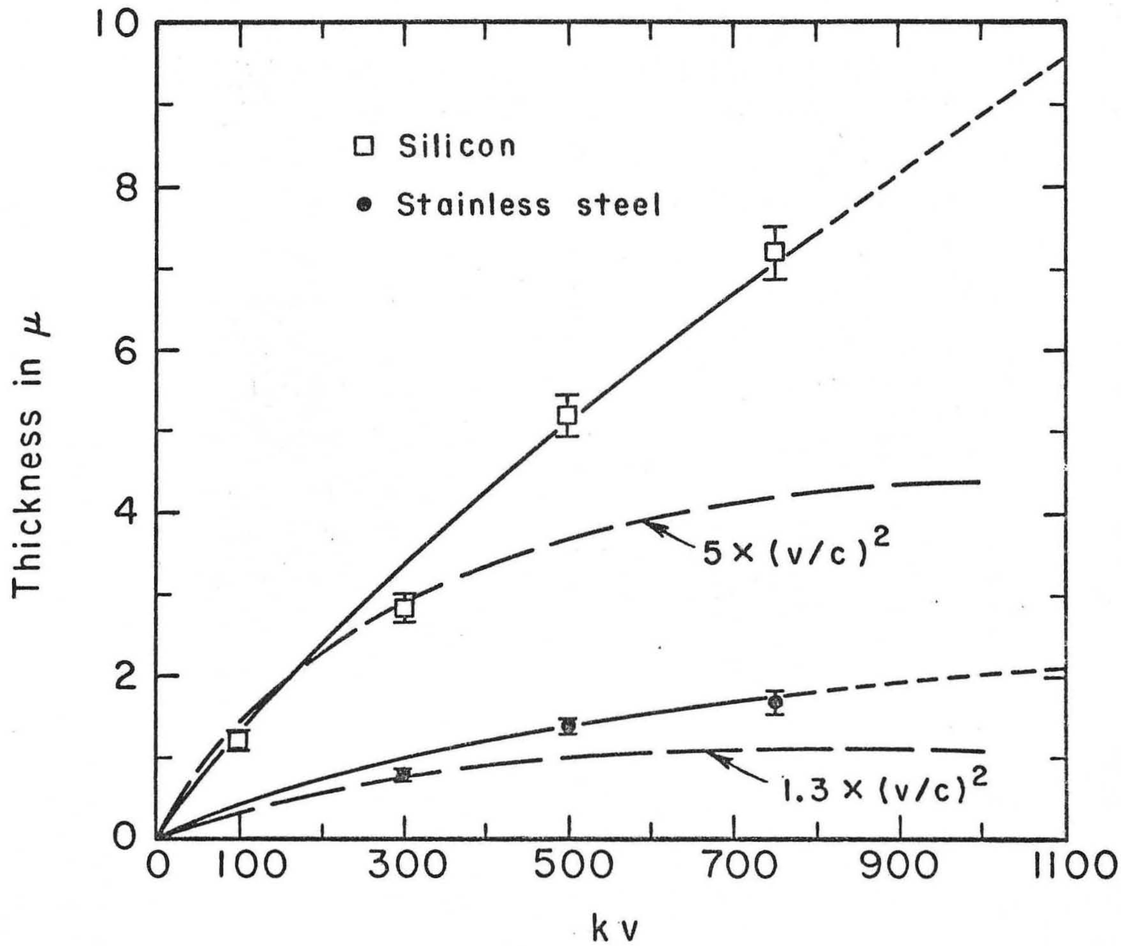

XBL679-5291

Fig. 4

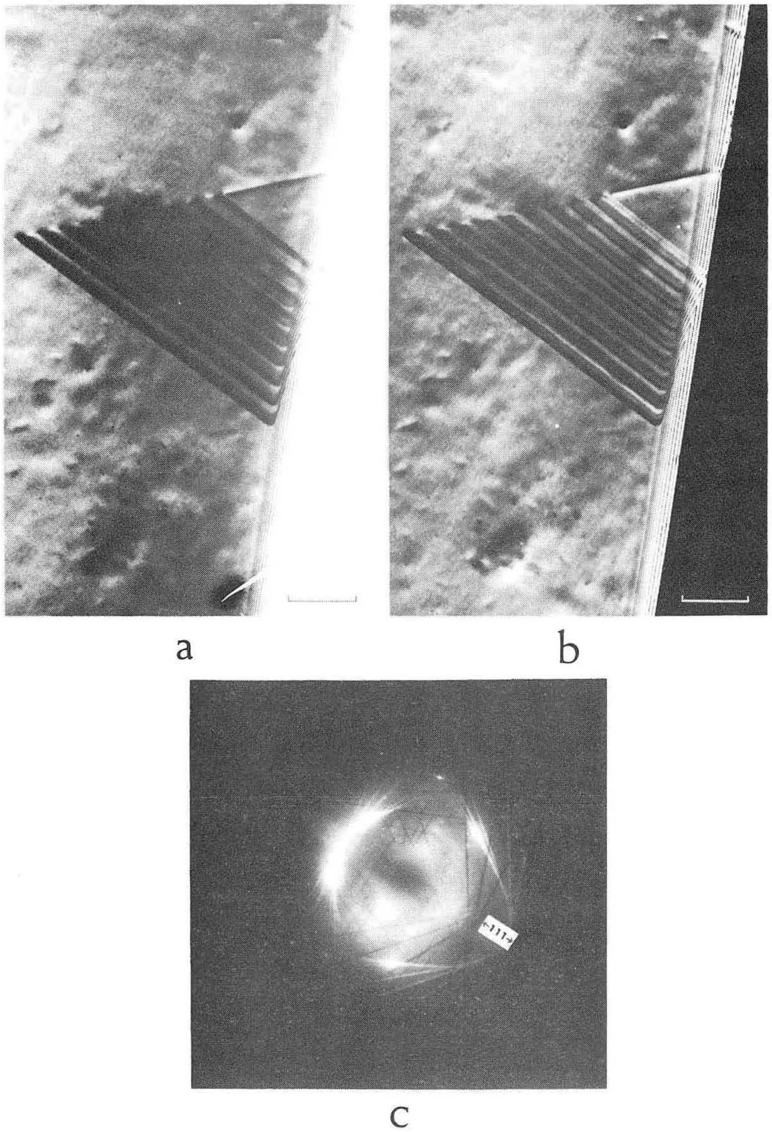

XBB 679-5631

Fig. 5

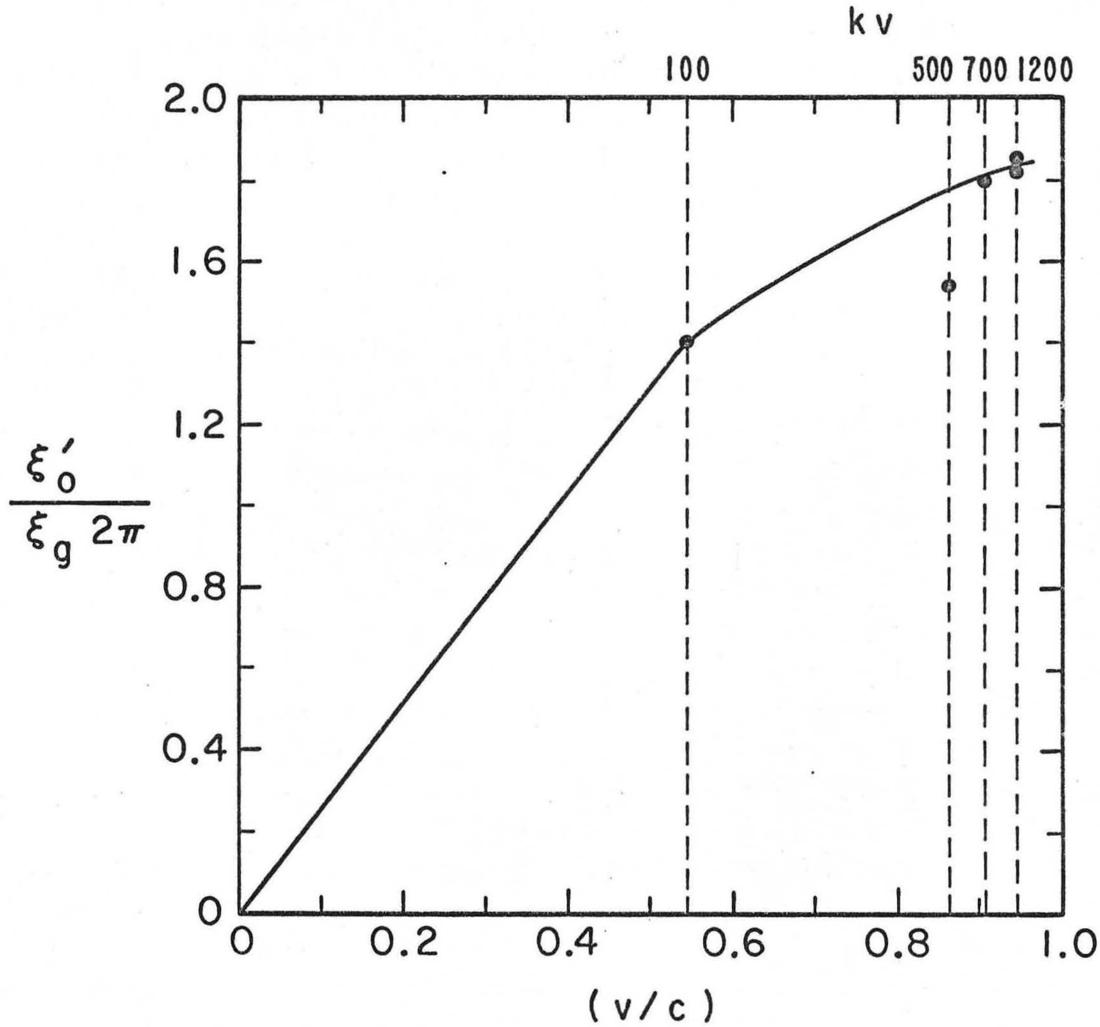

XBL679-5292

Fig. 6

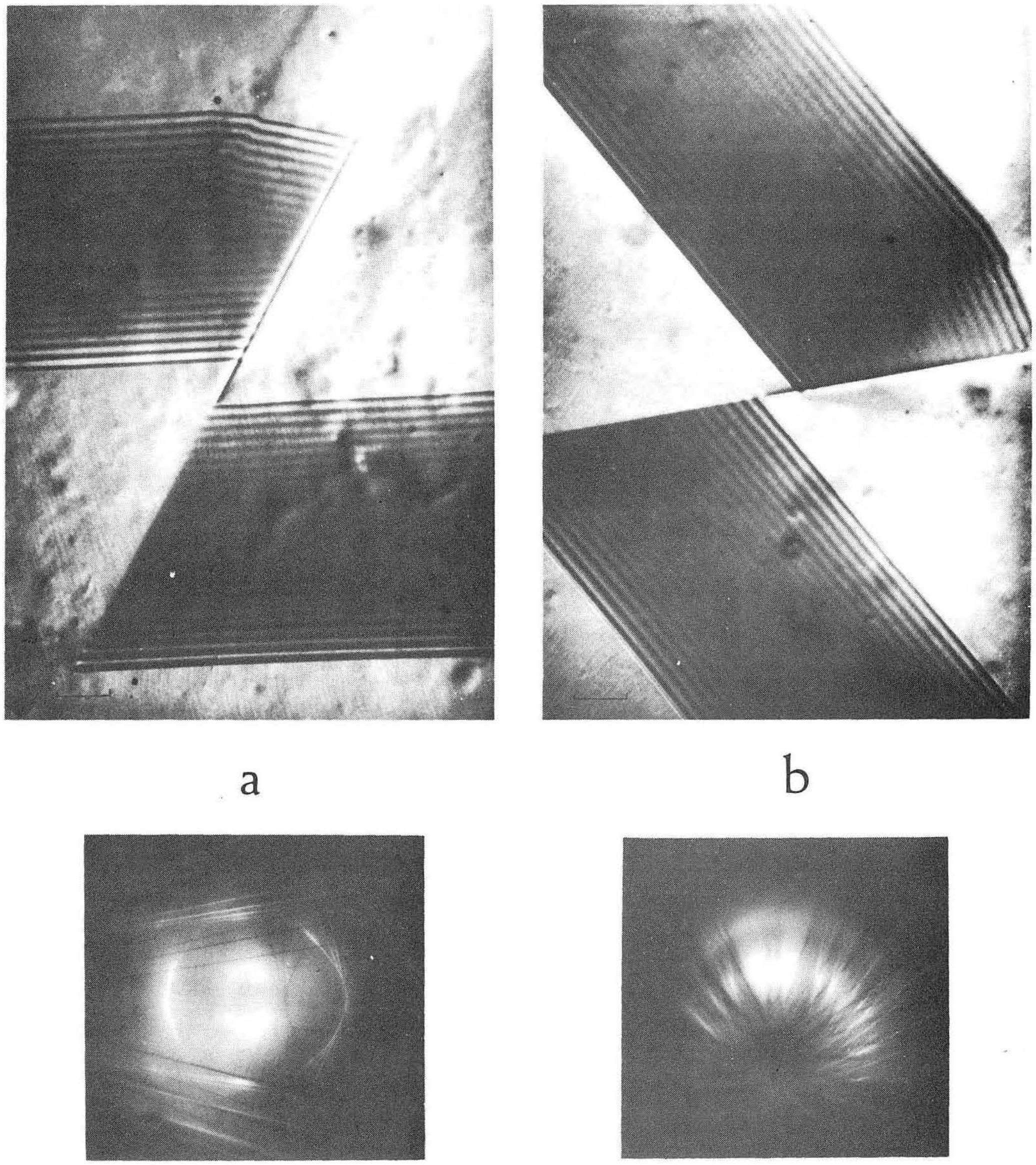

XBB 679-5635

Fig. 7

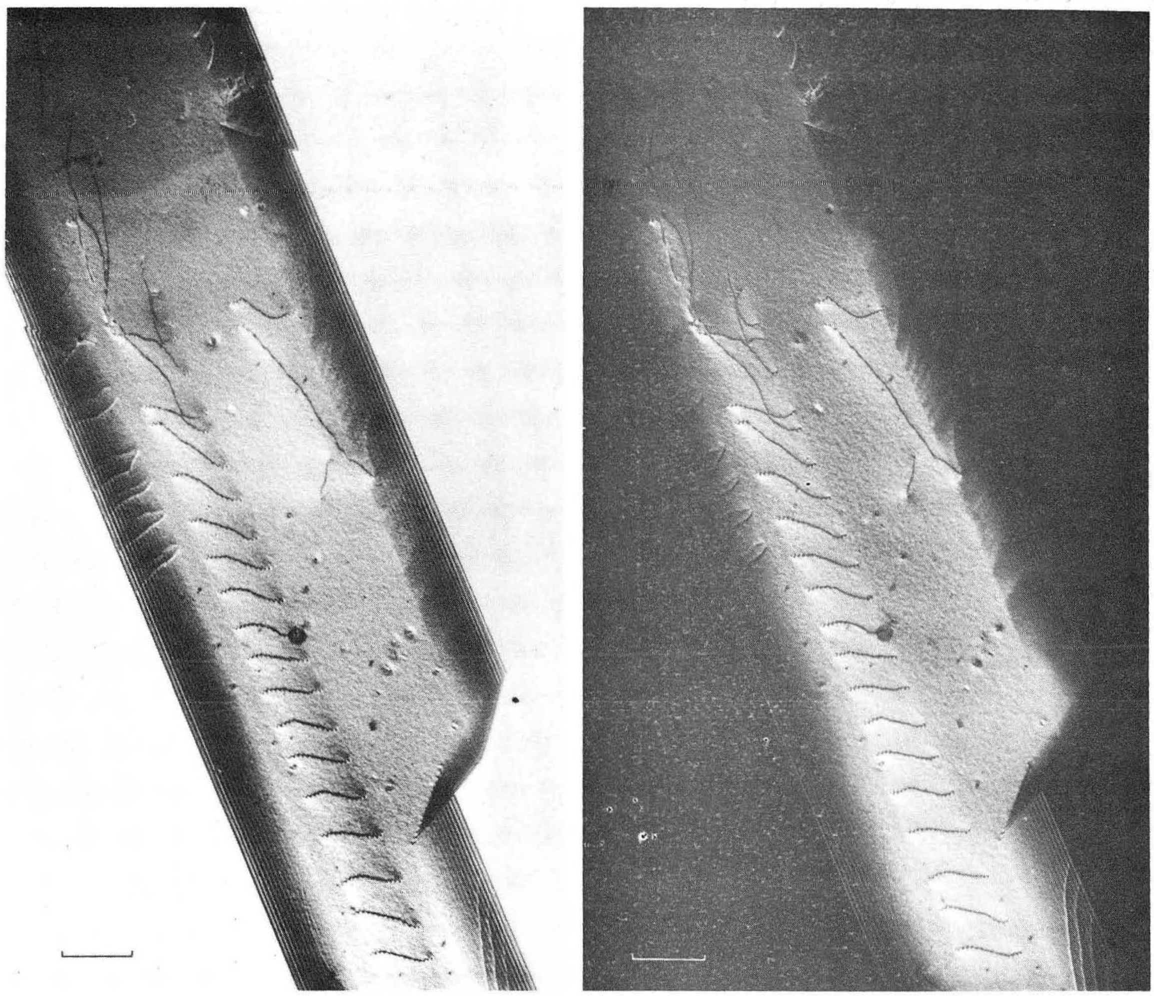

a b

XBB 679-5629

Fig. 8

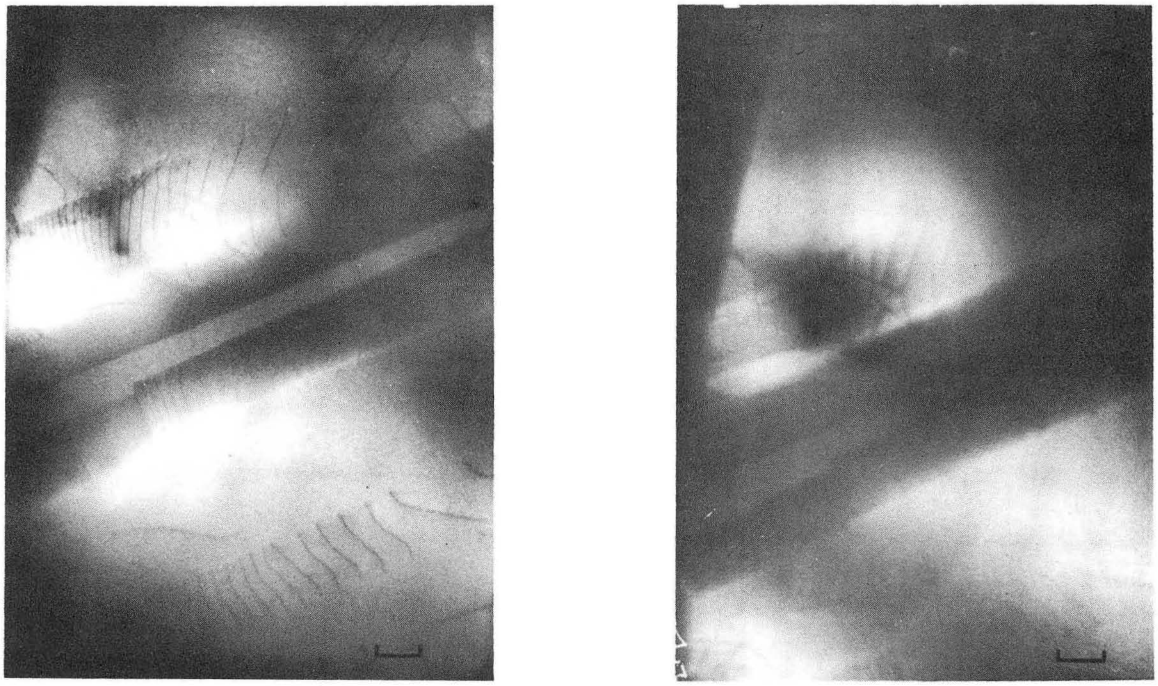

a b

XBB 679-5630

Fig. 9

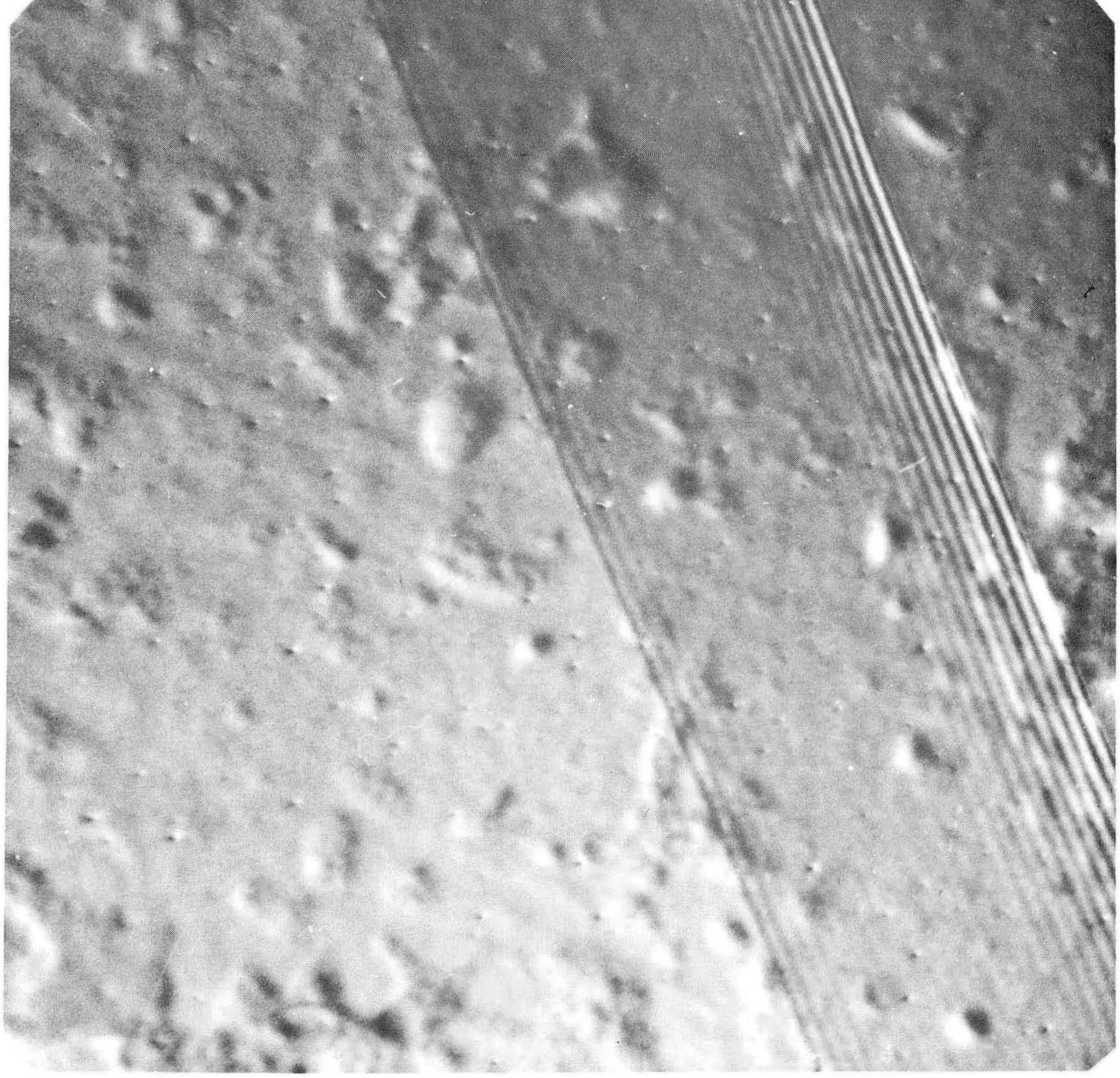

XBB 679-5628

Fig. 10

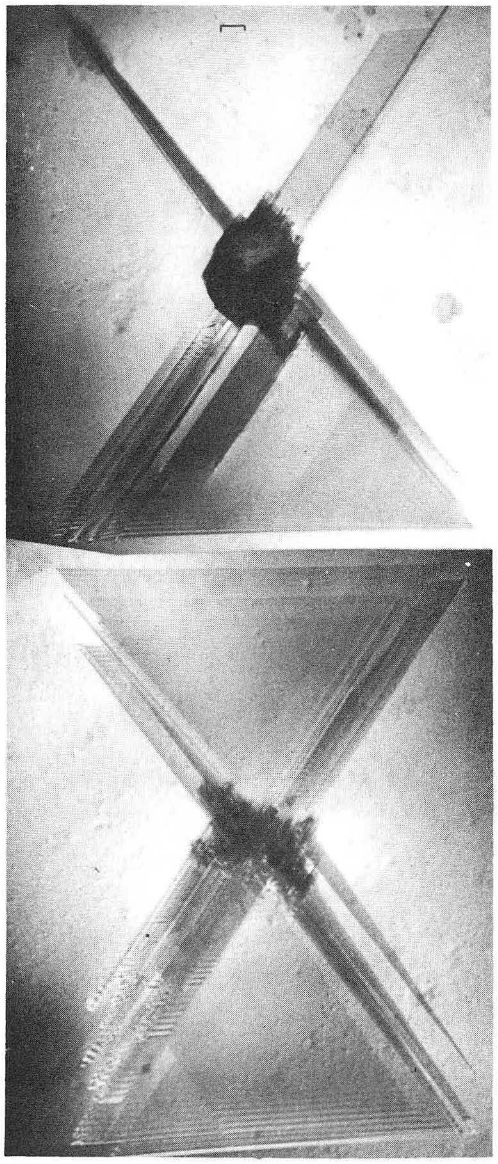

XBB 679-5633

Fig. 11